

# Specific heat and magnetic measurements in $\text{Nd}_{0.5}\text{Sr}_{0.5}\text{MnO}_3$ , $\text{Nd}_{0.5}\text{Ca}_{0.5}\text{MnO}_3$ and $\text{Ho}_{0.5}\text{Ca}_{0.5}\text{MnO}_3$ samples

J. López and O. F. de Lima

*Instituto de Física Gleb Wataghin, Universidade Estadual de Campinas,  
UNICAMP, 13083-970, Campinas, SP, Brazil*

P. N. Lisboa-Filho and F. M. Araujo-Moreira

*Depto. de Física, Universidade Federal de São Carlos, CP-676, São Carlos, SP, 13565-905, Brazil*

## Abstract

We studied the magnetization as a function of temperature and magnetic field in the compounds  $\text{Nd}_{0.5}\text{Sr}_{0.5}\text{MnO}_3$ ,  $\text{Nd}_{0.5}\text{Ca}_{0.5}\text{MnO}_3$  and  $\text{Ho}_{0.5}\text{Ca}_{0.5}\text{MnO}_3$ . It allowed us to identify the ferromagnetic, antiferromagnetic and charge ordering phases in each case. The intrinsic magnetic moments of  $\text{Nd}^{3+}$  and  $\text{Ho}^{3+}$  ions experienced a short range order at low temperatures. We also did specific heat measurements with applied magnetic fields between 0 and 9 T and temperatures between 2 and 300 K in all three samples. Close to the charge ordering and ferromagnetic transition temperatures the specific heat curves showed peaks superposed to the characteristic response of the lattice oscillations. Below 10 K the specific heat measurements evidenced a Schottky-like anomaly for all samples. However, we could not successfully fit the curves to either a two level nor a distribution of two-level Schottky anomaly. Our results indicated that the peak temperature of the Schottky anomaly was higher in the compounds with narrower conduction band.

60, 70, 65.40Ba, 74.25 Ha, 75.60.-d

Typeset using REVTeX

## I. INTRODUCTION

Compounds like  $\text{La}_{0.5}\text{Ca}_{0.5}\text{MnO}_3$  and  $\text{Nd}_{0.5}\text{Sr}_{0.5}\text{MnO}_3$  present a real-space ordering of  $\text{Mn}^{3+}$  and  $\text{Mn}^{4+}$  ions, named as charge ordering (CO). Close to the charge ordering temperature ( $T_{CO}$ ), these materials show anomalies in resistivity, magnetization and lattice parameters as a function of temperature, magnetic field and isotope mass<sup>1,2</sup>. At low temperatures both, ferromagnetic and antiferromagnetic phases, could coexist<sup>3</sup>. However, a relatively small external magnetic field can destroy the CO phase and enforces a ferromagnetic orientation of the spins<sup>4</sup>.

Moreover, electron microscope analysis has revealed convincing evidence that CO is accompanied by orientational ordering of the  $3d^3$  orbitals on the  $\text{Mn}^{3+}$  ions, called orbital ordering (OO)<sup>5</sup>. The physical properties in CO manganese perovskites are thought to arise from the strong competition among a ferromagnetic double exchange interaction, an antiferromagnetic superexchange interaction, and the spin-phonon coupling. These interactions are determined by intrinsic parameters such as doping level, average cationic size, cationic disorder and oxygen stoichiometry. Microscopically, CO compounds are particularly interesting because spin, charge and orbital degrees of freedom are at play simultaneously and classical simplifications that neglect some of these interactions do not work. More detailed information on the physics of manganites can be found in a review paper by Myron B. Salamon and Marcelo Jaime<sup>6</sup>.

We have shown that polycrystalline samples of  $\text{La}_{0.5}\text{Ca}_{0.5}\text{MnO}_3$  and  $\text{Nd}_{0.5}\text{Sr}_{0.5}\text{MnO}_3$  presented an unusual magnetic relaxation behavior close to each critical temperature<sup>7,8</sup>. However, a clear understanding of all these features has not been reached yet. An alternative to a bulk characterization like magnetization would be to perform specific heat measurements. In contrast to magnetization, which has a vector character, the specific heat is a scalar. Therefore, a comparison between both types of data could give valuable information.

J. E. Gordon et al.<sup>9</sup> reported specific heat measurements for a  $\text{Nd}_{0.67}\text{Sr}_{0.33}\text{MnO}_3$  sample and found a Schottky-like anomaly at low temperatures. They associated this result to the

magnetic ordering of  $\text{Nd}^{3+}$  ions and the crystal-field splitting at low temperature. F. Bar-tolomé et al.<sup>10</sup> also found Schottky-like anomaly in a closely related compound of  $\text{NdCrO}_3$ . They proposed a crystal-field energy level scheme in agreement with neutron-scattering studies in the same sample. In two papers V. N. Smolyaninova et al.<sup>11,12</sup> studied the low temperature specific heat in  $\text{Pr}_{1-x}\text{Ca}_x\text{MnO}_3$  ( $0.3 < x < 0.5$ ) and  $\text{La}_{1-x}\text{Ca}_x\text{MnO}_3$  ( $x=0.47, 0.5$  and  $0.53$ ). They found an excess specific heat,  $C'(T)$ , of non-magnetic origin associated with charge ordering. They also reported that a magnetic field sufficiently high to induce a transition from the charge ordered state to the ferromagnetic metallic state did not completely remove  $C'(T)$ . However, no Schottky anomaly was found in any of these compounds.

Here, we report magnetic and specific heat measurements with applied magnetic fields between 0 and 9 T and temperatures between 2 and 300 K for  $\text{Nd}_{0.5}\text{Sr}_{0.5}\text{MnO}_3$ ,  $\text{Nd}_{0.5}\text{Ca}_{0.5}\text{MnO}_3$  and  $\text{Ho}_{0.5}\text{Ca}_{0.5}\text{MnO}_3$  samples. All these compounds presented a Schottky-like anomaly at low temperatures, as well as characteristic peaks associated to the charge ordered, antiferromagnetic and/or ferromagnetic transitions. We have already reported a short version of preliminary results about these topics<sup>13</sup>. However, as far as we know, detailed specific heat measurements in these compounds have not been published.

## II. EXPERIMENTAL METHODS

Polycrystalline samples of  $\text{Nd}_{0.5}\text{Sr}_{0.5}\text{MnO}_3$ ,  $\text{Nd}_{0.5}\text{Ca}_{0.5}\text{MnO}_3$  and  $\text{Ho}_{0.5}\text{Ca}_{0.5}\text{MnO}_3$  were prepared by the sol-gel method<sup>14</sup>. Stoichiometric parts of  $\text{Nd}_2\text{O}_3$  ( $\text{Ho}_2\text{O}_3$ ) and  $\text{MnCO}_3$  were dissolved in  $\text{HNO}_3$  and mixed to an aqueous citric acid solution, to which  $\text{SrCO}_3$  or  $\text{CaCO}_3$  was added. The mixed metallic citrate solution presented the ratio citric acid/metal of 1/3 (in molar basis). Ethylene glycol was added to this solution, to obtain a citric acid/ethylene glycol ratio 60/40 (mass ratio). The resulting solution was neutralized to  $\text{pH} \sim 7$  with ethylenediamine. This solution was turned into a gel, and subsequently decomposed to a solid by heating at 400 °C. The resulting powder was heat-treated in vacuum at 900 °C for 24 hours, with several intermediary grindings, in order to prevent formation of

impurity phases. This powder was pressed into pellets and sintered in air at 1050 °C for 12 hours. X-ray diffraction measurements indicated high quality samples in all cases.

The magnetization measurements were done with a Quantum Design MPMS-5S SQUID magnetometer. Specific heat measurements were done with a Quantum Design PPMS calorimeter. The PPMS used the two relaxation time technique, and data was always collected during sample cooling. The intensity of the heat pulse was calculated to produce a variation in the temperature bath between 0.5 % (at low temperatures) and 2% (at high temperatures). Experimental errors during the specific heat and magnetization measurements were lower than 1 % for all temperatures and samples.

### III. RESULTS AND DISCUSSION

#### A. Magnetization measurements

Figure 1 shows the temperature dependence of magnetization, measured with a 5 T applied magnetic field and zero field cooling conditions, in polycrystalline samples of  $\text{Nd}_{0.5}\text{Sr}_{0.5}\text{MnO}_3$ ,  $\text{Nd}_{0.5}\text{Ca}_{0.5}\text{MnO}_3$  and  $\text{Ho}_{0.5}\text{Ca}_{0.5}\text{MnO}_3$ . All three compounds present a charge ordering transition below 160, 250 and 271 K, respectively<sup>15,16,17</sup>. It is interesting to note that the relation between the charge ordering temperature and the antiferromagnetic ordering temperature changes from one sample to the other. In the first case they are approximately coincident ( $T_{CO} \approx T_N$ ), in the second case the charge ordering temperature is much higher ( $T_{CO} \gg T_N$ ), and in the third case there is not a long range antiferromagnetic transition.

The  $\text{Nd}_{0.5}\text{Sr}_{0.5}\text{MnO}_3$  sample presents a ferromagnetic transition at  $T_C=250$  K and an antiferromagnetic transition at  $T_N=160$  K. The  $\text{Nd}_{0.5}\text{Ca}_{0.5}\text{MnO}_3$  compound presents a strong maximum near  $T_{CO}$ , but shows an unexpected minimum close to the antiferromagnetic transition temperature  $T_N=160$  K. Usually an antiferromagnetic transition is accompanied by a maximum in the temperature dependence of the magnetization. For temperatures lower

than 20 K both  $\text{Nd}_{0.5}\text{Sr}_{0.5}\text{MnO}_3$  and  $\text{Nd}_{0.5}\text{Ca}_{0.5}\text{MnO}_3$  samples show a sharp increase in the magnetization. This sharp increase in magnetization have been associated to a short range magnetic ordering of the intrinsic magnetic moment of  $\text{Nd}^{3+}$  ions<sup>18</sup>. However, no long range ferromagnetic order of the  $\text{Nd}^{3+}$  ions was found in neutron diffraction measurements at these low temperatures<sup>15,16</sup>.

Differently from the two previous samples, the  $\text{Ho}_{0.5}\text{Ca}_{0.5}\text{MnO}_3$  compound do not present a strong maximum at the charge ordering temperature in the magnetization versus temperature curve. The existence of charge ordering in  $\text{Ho}_{0.5}\text{Ca}_{0.5}\text{MnO}_3$  was suggested by T. Terai et al.<sup>17</sup> studying simultaneously the magnetization and resistivity curves. Figure 2 shows the inverse of the DC susceptibility measured with 0.1 mT (inset) and 5 T (main figure) in the  $\text{Ho}_{0.5}\text{Ca}_{0.5}\text{MnO}_3$  sample. The measurement at 5 T clearly indicates a transition between two linear behaviors near 270 K. This latter result, together with the specific heat measurements, that we will discuss below, reinforces the idea of the existence of a charge ordering transition in the  $\text{Ho}_{0.5}\text{Ca}_{0.5}\text{MnO}_3$  sample, although the details of the interactions in this compound differ from those in  $\text{Nd}_{0.5}\text{Sr}_{0.5}\text{MnO}_3$  and  $\text{Nd}_{0.5}\text{Ca}_{0.5}\text{MnO}_3$ . On the other hand, the DC susceptibility measurement in  $\text{Ho}_{0.5}\text{Ca}_{0.5}\text{MnO}_3$  with a probe field of 0.1 mT indicates two possible Curie-Weiss intervals: below and above 100 K (see straight lines).

We fitted the magnetization data, measured with a probe field of 0.1 mT for all samples, to a Curie-Weiss law:  $M/H \sim \mu_{eff}^2/(T - T_\Theta)$ , where  $M/H$  was the DC susceptibility,  $\mu_{eff}$  was the effective paramagnetic moment and  $T_\Theta$  was the Curie-Weiss temperature. A simplified theoretical estimate<sup>16</sup> of the effective paramagnetic moment gives values of  $5.1 \mu_B$ ,  $5.1 \mu_B$  and  $8.7 \mu_B$  for  $\text{Nd}_{0.5}\text{Sr}_{0.5}\text{MnO}_3$ ,  $\text{Nd}_{0.5}\text{Ca}_{0.5}\text{MnO}_3$  and  $\text{Ho}_{0.5}\text{Ca}_{0.5}\text{MnO}_3$  samples, respectively. The positive or negative value of  $T_\Theta$  suggests the predominance of local ferromagnetic or antiferromagnetic interactions between the spins in the corresponding interval of temperature used. However, it is important to remember that the Curie-Weiss law is only a mean field approximation, that do not consider fluctuations.

In our case the fitting interval was taken between 300 and 400 K in the  $\text{Nd}_{0.5}\text{Sr}_{0.5}\text{MnO}_3$  and  $\text{Nd}_{0.5}\text{Ca}_{0.5}\text{MnO}_3$  samples. The  $\mu_{eff}$  and  $T_\Theta$  values were  $2.2 \mu_B$  and  $2.1 \mu_B$ , and 260 K

and 215 K for  $\text{Nd}_{0.5}\text{Sr}_{0.5}\text{MnO}_3$  and  $\text{Nd}_{0.5}\text{Ca}_{0.5}\text{MnO}_3$  samples, respectively. The discrepancies between our experimentally measured values of  $\mu_{eff}$  and the theoretical ones in the samples of  $\text{Nd}_{0.5}\text{Sr}_{0.5}\text{MnO}_3$  and  $\text{Nd}_{0.5}\text{Ca}_{0.5}\text{MnO}_3$ , are essentially due to the vicinity of the  $T_C$  or  $T_{CO}$  temperatures to the temperature interval that we could use to fit the curves to the Curie-Weiss law. F. Millange et al.<sup>16</sup> measured the effective paramagnetic moment, in the interval between 450 and 800 K, for a  $\text{Nd}_{0.5}\text{Ca}_{0.5}\text{MnO}_3$  sample and found a value roughly in agreement with theory. M. T. Causa et al.<sup>19</sup> also showed that the transition to a Curie-Weiss regime in several manganites occurs approximately for  $T > 2T_C$ . In the temperature interval approximately between  $2T_C$  and  $T_C$  magnetic ions start to form local clusters. This behavior is different from the one of a simple ferromagnetic sample like iron, where the transition from the ferromagnetic state to the Curie-Weiss regime occurs in a much shorter temperature interval.

For the  $\text{Ho}_{0.5}\text{Ca}_{0.5}\text{MnO}_3$  sample we fitted the Curie-Weiss law to two intervals: from 100 to 350 K and from 2 to 100 K. In the  $\text{Ho}_{0.5}\text{Ca}_{0.5}\text{MnO}_3$  sample the  $\mu_{eff}$  and  $T_\Theta$  values were  $9.7 \mu_B$  and  $3.4 \mu_B$ , and -38 K and -16 K for the high and low temperature intervals, respectively. The effective paramagnetic moment found in the high temperature interval for the  $\text{Ho}_{0.5}\text{Ca}_{0.5}\text{MnO}_3$  sample is roughly in agreement with the theoretical value, and the negative value of  $T_\Theta$  indicates that the main local interactions are antiferromagnetic. However, the transition approximately below 100 K to a different Curie-Weiss regime suggests that the predominance of short range antiferromagnetic interactions are giving space to short range ferromagnetic ones, with a higher value of  $T_\Theta$ . This conclusion is also supported by the magnetic field dependence of the magnetization, as we will discuss below.

Figure 3 shows the magnetization hysteresis cycle at 2 K for the three studied samples. The applied magnetic field was increased from 0 to 5 T, decreased to -5 T and then increased back to 5 T again. The  $\text{Nd}_{0.5}\text{Sr}_{0.5}\text{MnO}_3$  curve is characteristic of a mixture of two phases: one ferromagnetic and another antiferromagnetic. The ferromagnetic part is easily oriented at low magnetic field values and shows a hysteretical behavior. The almost linear and reversible dependence for magnetic fields higher than approximately 1 T, indicates a gradual

destruction of the antiferromagnetic phase<sup>8</sup>. R. Mahendiram et al.<sup>20</sup> reported, in a sample with the same composition at 50 K, that for magnetic fields higher than approximately 5 T, the magnetization started to increase rapidly, and for magnetic fields above 10 T, it slowly approached the ferromagnetic saturation value. Because at 2 K these transition fields are much higher than 5 T we were unable to see them. The  $\text{Nd}_{0.5}\text{Ca}_{0.5}\text{MnO}_3$  curve did not show any trace of a ferromagnetic component at low fields. In fact, the curve is linear and reversible for the whole magnetic field interval. As before, this linearity characterizes the gradual destruction of the antiferromagnetic phase. F. Millange et al.<sup>16</sup> reported, for a sample with the same composition, a set of M vs. H curves with applied magnetic fields up to 22 T. They found sharp transitions and a large hysteresis at 130 K, between applied magnetic fields of 12 and 18 T. Their results were interpreted as evidence of the existence of a spin-flop transition.

In the M vs. H curve for the  $\text{Ho}_{0.5}\text{Ca}_{0.5}\text{MnO}_3$  sample, two characteristics are well noticed. One, that there is not hysteresis at all, and second, that the magnetization values at 5 T are well below the theoretical saturation value of  $8.7 \mu_B$ . In order to try to discriminate between a paramagnetic or ferromagnetic ordering at 2 K, the experimental points were fitted by a Brillouin function<sup>21</sup>:

$$M = (N/V) \gamma J B_J(x) \quad (1)$$

where  $\gamma = g \mu_B$ ,  $\beta = 1/k_B T$  and

$$B_J(x) = [(2J + 1)/2J] \coth[(2J + 1)x/2J] - (1/2J) \coth(x/2J) \quad (2)$$

Here,  $x = \beta \gamma J H$ ,  $N/V$  is the number of ions per unit volume,  $g$  is an effective gyromagnetic ratio,  $J$  is the total angular momentum,  $T$  is the temperature,  $\mu_B$  is the Bohr magneton and  $k_B$  is the Boltzmann constant. Equation 1 is valid for a set of identical and not interacting ions of angular momentum  $J$ . Because our sample has three different magnetic ions we fixed  $J=8$  ( $\text{Ho}^{3+}$ ),  $J=2$  ( $\text{Mn}^{3+}$ ) or  $J=3/2$  ( $\text{Mn}^{4+}$ ) and let the effective gyromagnetic ratio to change freely in each case. The best fitting, represented by the solid line in figure 3, was

found for  $J=8$  and  $g=0.35$ . Although it is difficult to enunciate a more conclusive statement from these results, they suggest that there is not a long range ferromagnetic order for the  $\text{Ho}_{0.5}\text{Ca}_{0.5}\text{MnO}_3$  sample, at 2 K.

### B. Specific heat at high temperatures

Figure 4 shows specific heat measurements with a zero applied magnetic field from 2 to 300 K in the  $\text{Nd}_{0.5}\text{Sr}_{0.5}\text{MnO}_3$ ,  $\text{Nd}_{0.5}\text{Ca}_{0.5}\text{MnO}_3$  and  $\text{Ho}_{0.5}\text{Ca}_{0.5}\text{MnO}_3$  samples. In order to facilitate the visualization, the curves for  $\text{Nd}_{0.5}\text{Sr}_{0.5}\text{MnO}_3$  and  $\text{Ho}_{0.5}\text{Ca}_{0.5}\text{MnO}_3$  were displaced 20 J/mol K upside and downside, respectively. Specific heat measurements give information about both lattice and magnetic excitations. At high temperatures the excitations from the lattice vibrations are dominant and decrease as the temperature decreases. The magnetic contribution can be obtained by subtracting the lattice part from the experimental values.

The Dulong and Petit<sup>22</sup> model predicts that the thermal contribution at high temperature increases asymptotically to the value  $C_{DP} = 3nR$ , where  $n$  is the number of atoms in the compound's formulae and  $R$  is the ideal gas constant. Therefore,  $C_{DP} = 125$  J/(mol K) for all studied samples in this work, since their unit cell contain 5 atoms each. At 300 K the experimental specific heat values were 110 J/(mol K) (88 % of  $C_{DP}$ ) for the  $\text{Nd}_{0.5}\text{Sr}_{0.5}\text{MnO}_3$  and  $\text{Nd}_{0.5}\text{Ca}_{0.5}\text{MnO}_3$  samples and 100 J/(mol K) (80 % of  $C_{DP}$ ) for the  $\text{Ho}_{0.5}\text{Ca}_{0.5}\text{MnO}_3$  sample. These values suggest that the Debye temperature should be, within the experimental error, approximately equal for all three compounds.

Continuous lines in figure 4 represent the fitting of the thermal background, in the interval from 30 to 300 K, by the Einstein model given by:

$$C_{Einstein} = 3nR \sum_i a_i \left[ \frac{x_i^2 e^{x_i}}{(e^{x_i} - 1)^2} \right] \quad (3)$$

where  $x_i = T_i/T$ . We used three optical phonons ( $i = 1, 2, 3$ ) with energies  $T_i$  (in Kelvin) and relative occupations  $a_i$ . The Einstein model for the specific heat considers the oscillation frequency (or energy) independently from the wave vector, which is a valid approximation

for the optical part of the spectrum. The values of temperatures (energies) found were 148, 438 and 997 K for  $\text{Nd}_{0.5}\text{Sr}_{0.5}\text{MnO}_3$ , 152, 432 and 1035 K for  $\text{Nd}_{0.5}\text{Ca}_{0.5}\text{MnO}_3$  and 147, 438 and 1023 K for  $\text{Ho}_{0.5}\text{Ca}_{0.5}\text{MnO}_3$ . These values are similar to those reported, using the same model, by A. P. Ramirez et al.<sup>23</sup> in a  $\text{La}_{0.37}\text{Ca}_{0.63}\text{MnO}_3$  sample and Raychaudhuri et al.<sup>24</sup> in a  $\text{Pr}_{0.63}\text{Ca}_{0.37}\text{MnO}_3$  sample. However, we should point out that the values found are not unique because there are six varying parameters during the fitting (one energy and one occupation coefficient for each oscillation mode).

An alternative method to determine the oscillation mode energies of the crystalline lattice is to study the Raman spectrum of a given compound. For example, V. Dediu et al.<sup>25</sup> found that, at a measured temperature of 50 K for a  $\text{Pr}_{0.65}\text{Ca}_{0.35}\text{MnO}_3$  sample, the strongest peaks were located at energies of 683 and 877 K. Besides, E. Granado et al.<sup>26</sup> found that, at a measured temperature of 200 K for a  $\text{Nd}_{0.66}\text{Ca}_{0.33}\text{MnO}_3$  sample, the strongest peaks were located at energies of 388, 439, 690 and 877 K. However, these peaks were not the only ones, they could change with temperature and they are not narrow. Furthermore, the Raman spectrum could depend on variables like the frequency, the intensity of the excitation laser and the luminosity of the sample. All of these make difficult a straightforward comparison between both methods to determine the oscillation energies of a crystalline lattice.

Figure 5 represents the differences between the experimental data and the fitted curves in figure 4. There is a maximum at 231 K for the  $\text{Nd}_{0.5}\text{Sr}_{0.5}\text{MnO}_3$  sample, which is correlated with the ferromagnetic transition at 250 K in the corresponding magnetization curve (figure 1). A second maximum, which could be partially associated to the antiferromagnetic and charge ordering transitions at 160 K, appears at 180 K. However, lattice parameters in this compound change rapidly between approximately 110 K and 250 K<sup>27</sup>. This variation in lattice parameters changes the intensity of the interactions between the atoms, and consequently the oscillation frequency of the phonons mode, contributing to the specific heat in the second peak. Figure 5 also shows that there is a maximum at 243 K for the  $\text{Nd}_{0.5}\text{Ca}_{0.5}\text{MnO}_3$  sample. This maximum correlates with the corresponding charge ordering temperature at 250 K. Differently from the  $\text{Nd}_{0.5}\text{Sr}_{0.5}\text{MnO}_3$  sample, there is not magnetic

ordering in this high temperature interval for the  $\text{Nd}_{0.5}\text{Ca}_{0.5}\text{MnO}_3$  sample. In this latter compound lattice parameters change very rapidly between approximately 200 and 250 K<sup>16</sup>. An inflection point in the  $C$  vs.  $T$  curve appears at 141 K for the  $\text{Nd}_{0.5}\text{Ca}_{0.5}\text{MnO}_3$  sample. Besides, there is a maximum at 141 K in figure 5, but its height is relatively small compared to the maximum at 243 K. The Neel temperature corresponding to this compound is 160 K. Therefore, these results lead us to conclude that the specific heat variations due to the antiferromagnetic order are small compared to those induced in the charge ordering and ferromagnetic transitions. For the  $\text{Ho}_{0.5}\text{Ca}_{0.5}\text{MnO}_3$  sample, we found a maximum at 276 K. This maximum is correlated with the transition seen at high magnetic fields in the inverse DC susceptibility curve of figure 2. These experimental results and the resistivity measurements reported by T. Terai et al.<sup>17</sup>, indicate the existence of a phase transition between 270 and 280 K. However, electron diffraction studies would be needed to unambiguously classify this transition as CO.

V. Hardy et al.<sup>28</sup> reported similar measurements in a single crystal of  $\text{Pr}_{0.63}\text{Ca}_{0.37}\text{MnO}_3$ . They found a specific heat peak at 229 K and resistivity and magnetization curves indicated a charge ordering transition at 227 and 228 K, respectively. They also point out that part of the peak amplitude was due to the crystalline lattice distortions. Moreover, the specific heat curve showed an inflection point at 150 K, close to the corresponding  $T_N = 160$  K. Similar characteristics were also found in a polycrystalline sample of  $\text{La}_{0.37}\text{Ca}_{0.63}\text{MnO}_3$ <sup>23</sup>.

Results in figure 5 allow us to calculate the variation in entropy ( $\Delta S$ ), associated to the charge ordering, ferromagnetic and antiferromagnetic transitions:

$$\Delta S = \int_{T_i}^{T_f} \frac{(C - C_{ph})}{T} dT \quad (4)$$

where  $T_i$  and  $T_f$  are two temperatures conveniently chosen to delimitate the interval of interest and  $C_{ph}$  is the specific heat due to the lattice oscillations.

For the  $\text{Nd}_{0.5}\text{Ca}_{0.5}\text{MnO}_3$  sample the entropy variation between 201 and 301 K was  $\Delta S(T_{CO}) = 2.0$  J/(mol K). A. K. Raychaudhuri et al.<sup>24</sup> reported an entropy variation, close to the charge ordering transition in the compound  $\text{Pr}_{0.63}\text{Ca}_{0.37}\text{MnO}_3$ , of 1.8 J/(mol K)

with zero applied magnetic field and 1.5 J/(mol K) with an 8 T magnetic field. On the other hand, Ramirez et al.<sup>23</sup> found  $\Delta S(T_{CO}) = 5$  J/(mol K) in a  $\text{La}_{0.37}\text{Ca}_{0.63}\text{MnO}_3$  sample. All these results correspond to those expected for a charge ordering transition<sup>24</sup>. On the other hand, the entropy variation (not related with phonons), calculated between 118 and 201 K for the  $\text{Nd}_{0.5}\text{Ca}_{0.5}\text{MnO}_3$  sample, was  $\Delta S(T_N) = 0.80$  J/(mol K). We associate this smaller  $\Delta S$  value to the antiferromagnetic order at  $T_N = 160$  K.

The entropy variation between 133 and 274 K for the  $\text{Nd}_{0.5}\text{Sr}_{0.5}\text{MnO}_3$  sample was  $\Delta S(T_{CO+FM}) = 3.6$  J/(mol K). Considering that the entropy variation associated to the charge ordering transition is the same as for the  $\text{Nd}_{0.5}\text{Ca}_{0.5}\text{MnO}_3$  sample, we found that the entropy variation associated to the ferromagnetic transition is approximately 1.6 J/(mol K). Using a model proposed by J. E. Gordon et al.<sup>9</sup> we estimated that the change in entropy needed to a full ferromagnetic transition in the  $\text{Nd}_{0.5}\text{Sr}_{0.5}\text{MnO}_3$  sample was 12.45 J/(mol K). Therefore, the fact that the entropy variation found is 13 % of the theoretical value, confirms that only a small part of the spins order ferromagnetically. The same report of J. E. Gordon et al.<sup>9</sup> found that the entropy variation associated to the ferromagnetic order in a  $\text{Nd}_{0.67}\text{Sr}_{0.33}\text{MnO}_3$  sample was approximately 10 % of the theoretical value. The entropy variation, not associated to lattice oscillations, between 216 and 294 K for the  $\text{Ho}_{0.5}\text{Ca}_{0.5}\text{MnO}_3$  sample was  $\Delta S(T_{CO}) = 0.78$  J/(mol K). This  $\Delta S(T_{CO})$  for the  $\text{Ho}_{0.5}\text{Ca}_{0.5}\text{MnO}_3$  sample is smaller than the corresponding value for the  $\text{Nd}_{0.5}\text{Ca}_{0.5}\text{MnO}_3$  sample, suggesting a different nature of the charge ordering transition.

### C. Specific heat at low temperatures

For temperatures lower than 30 K, the phonon contribution to the specific heat starts to take a smaller part, and the C vs. T curve shows a slow variation. Figure 6 reproduces the specific heat measurements for temperatures between 2 and 30 K in the samples of (a)  $\text{Nd}_{0.5}\text{Sr}_{0.5}\text{MnO}_3$ , (b)  $\text{Nd}_{0.5}\text{Ca}_{0.5}\text{MnO}_3$  and (c)  $\text{Ho}_{0.5}\text{Ca}_{0.5}\text{MnO}_3$ . Measurements were made in the presence of applied magnetic fields of 0 T (open squares), 5 T (closed circles), 7 T

(open up triangles) and 9 T (closed down triangles). Note that close to 5 K all curves show a Schottky-like anomaly<sup>22</sup>.

It is important to stress that high values of specific heat were found at low temperatures for the three samples presented here. These values are similar to those reported by J. E. Gordon et. al.<sup>9</sup> in a sample of  $\text{Nd}_{0.67}\text{Sr}_{0.33}\text{MnO}_3$ . However, the absolute values of specific heat at 2 K, reported by J. J. Hamilton et al.<sup>29</sup> in samples of  $\text{La}_{0.67}\text{Ba}_{0.33}\text{MnO}_3$  and  $\text{La}_{0.80}\text{Ca}_{0.20}\text{MnO}_3$ , were more than 100 times smaller. Similarly, V. Hardy et al.<sup>28</sup>, in a single crystal of  $\text{Pr}_{0.63}\text{Ca}_{0.37}\text{MnO}_3$ , found values approximately equal to those reported by J. J. Hamilton et al.<sup>29</sup>. The high values of specific heat found in our work could be interpreted as an increase in the effective mass of the electrons due to localization, which is also consistent with the insulating behavior revealed by electrical resistivity measurements<sup>15,16,17</sup>.

Continuous lines in figure 6 indicate the fitting of the experimental data between 15 and 30 K by the following expression<sup>9</sup>:

$$C = \sum \beta_{2n+1} T^{2n+1} \quad (5)$$

Here,  $C$  is the specific heat,  $T$  is the temperature and the parameters  $\beta_{2n+1}$  represent the contribution of the phonon modes. Notice that we did not include the lowest temperature interval to avoid the Schottky anomaly. To be able to fit the whole temperature interval we have chosen values of  $n$  from 1 to 4. Nonetheless, this large number of free parameters difficult an unique determination of each one. Since from resistivity measurements<sup>32,16,17</sup> all the studied samples show an insulating behavior at low temperatures, and the applied magnetic fields are not strong enough to destroy this characteristic, the expected linear contribution, from the free electrons to the specific heat, is zero. However, other kind of excitations could lead to a linear contribution. This can imply an implicit error of the fitting model. Moreover, we could not resolve in our data a term of type  $T^{3/2}$ . This term is usually interpreted as an evidence of the existence of ferromagnetic interactions. However, previous studies in samples clearly identified by other techniques as ferromagnetic, have not found this term in the specific heat either<sup>12,29</sup>.

The values of  $\beta_3$  change between 0.28 mJ/(mol K<sup>4</sup>) at H=0 T in Nd<sub>0.5</sub>Sr<sub>0.5</sub>MnO<sub>3</sub> to 1.57 mJ/(mol K<sup>4</sup>) at H=5 T in Ho<sub>0.5</sub>Ca<sub>0.5</sub>MnO<sub>3</sub>. The corresponding Debye temperatures ( $T_D$ ), obtained from  $\beta_3$ , will be plotted in figure 7a. The graphs in the insets of figure 6 show the differences between the specific heat experimental data and the phonon contribution to the specific heat, extrapolated to low temperatures from the fitting in the temperature interval between 15 and 30 K.

Figure 7 shows (a) the magnetic field dependence of the Debye temperature, (b) the variation of magnetic entropy between 2 and 20 K ( $\Delta S$ ) and (c) the Schottky temperature ( $T_S$ ) in the three studied samples. The entropy variation was calculated from equation 4 and the Schottky temperature was determined from the maxima in the insets of figure 6.

The Debye temperature was calculated using the values of  $\beta_3$  and the following equation<sup>22</sup>:

$$T_D = \left( \frac{12\pi^4 nR}{5\beta_3} \right)^{1/3} \quad (6)$$

where  $n$  is the number of atoms in the unit cell and  $R$  is the ideal gas constant. We should point out that the Debye temperature was estimated from the low temperature data. This procedure lead to a Debye temperature that is slightly different than the actual value of temperature for which the specific heat saturates. The Debye temperature from the low temperature data decreases with the increase of the applied magnetic field. We have also made specific heat measurements with a 9 T magnetic field, at high temperatures, for several charge ordered compounds<sup>30</sup>, and they show an increase of the specific heat when compared to the 0 T case, in agreement with the magnetic field dependence of the Debye temperatures. Other authors<sup>9</sup> have made an initial assumption that the Debye temperature is magnetic field independent, which is not supported by our experimental results.

Figure 7 also shows that  $T_S$  grows with the increase of the external magnetic field in all cases. However, the growth of  $T_S$  seems to be saturated for a magnetic field of 5 T in the sample of Ho<sub>0.5</sub>Ca<sub>0.5</sub>MnO<sub>3</sub>, while there is no sign of  $T_S$  saturation in the other two compounds. It is also interesting to note here the relative low  $T_S$  values. For the reagent compounds of Nd<sub>2</sub>O<sub>3</sub> and Ho<sub>2</sub>O<sub>3</sub> the peak in the specific heat, measured in zero magnetic

field, were found at approximately 10 and 9 K, respectively<sup>31</sup>. The fact that  $T_S$  is lower in the manganese compounds suggests that the collective charge ordered phase could be determining a smaller splitting in the energy levels.

The entropy variation, associated to the Schottky anomaly, grows as a function of magnetic field in the sample of  $\text{Nd}_{0.5}\text{Sr}_{0.5}\text{MnO}_3$ . The same result is clearly visualized from the height of the Schottky anomaly in the inset of figure 6a. J. E. Gordon et al.<sup>9</sup> also reported a similar increase in a sample of  $\text{Nd}_{0.67}\text{Sr}_{0.33}\text{MnO}_3$ . However, the Schottky entropy variation decreases with the increase of magnetic field in the  $\text{Nd}_{0.5}\text{Ca}_{0.5}\text{MnO}_3$  and  $\text{Ho}_{0.5}\text{Ca}_{0.5}\text{MnO}_3$  samples. In these two cases, the  $C$  vs.  $T$  curves in figure 6b and 6c, indicate that the local minimum, at a temperature above the Schottky anomaly, disappears with the increase of the external magnetic field. This is also reflected in the decrease of the height of the peak with the increase of the applied magnetic field (insets of figures 6b and 6c). These results seem to indicate that the magnetic field dependence of the Schottky anomaly is more correlated with the presence ( $\text{Nd}_{0.5}\text{Sr}_{0.5}\text{MnO}_3$ ) or not ( $\text{Nd}_{0.5}\text{Ca}_{0.5}\text{MnO}_3$  and  $\text{Ho}_{0.5}\text{Ca}_{0.5}\text{MnO}_3$ ) of ferromagnetic interactions than with the particular type of magnetic ion ( $\text{Nd}^{3+}$  or  $\text{Ho}^{3+}$ ).

The expected entropy variation from the magnetic ordering of  $\text{Nd}^{3+}$  or  $\text{Ho}^{3+}$  ions could be estimated<sup>9</sup> as  $\Delta S = 0.5 R \ln(2)$ , where  $R$  is the ideal gas constant. The actually found variation correspond to values from 63 to 77 % of the expected ones in the  $\text{Nd}_{0.5}\text{Sr}_{0.5}\text{MnO}_3$  sample, 80 to 62 % in the  $\text{Nd}_{0.5}\text{Ca}_{0.5}\text{MnO}_3$  sample and 68 to 25 % in the  $\text{Ho}_{0.5}\text{Ca}_{0.5}\text{MnO}_3$  sample, for magnetic fields between 0 and 9 T, respectively. J. E. Gordon et al.<sup>9</sup> found that the entropy variation associated to the ordering of  $\text{Nd}^{3+}$  ions in  $\text{Nd}_{0.67}\text{Sr}_{0.33}\text{MnO}_3$  was approximately 85 % of the expected value.

Let us consider that Nd (Ho) ions be oriented by a molecular field interaction ( $H_{mf}$ ), and not by the exchange interaction between pairs of Nd-Nd ions (Ho-Ho)<sup>9</sup>. Assuming that  $H_{mf}$  does not change with the external magnetic field, it is possible to estimate it, using a mean field model and the peak temperature in the specific heat. Considering a two level energy splitting  $\Delta(H)$ , due to a magnetic moment  $m$  in an external magnetic field  $H$ , one finds in zero applied field  $\Delta(0) = 2mH_{mf}$ , and in  $H = 9$  T the value changes to

$\Delta(9 \text{ T}) = 2m[H_{mf} + 9 \text{ T}]$ . One can also use that the energy splitting could be related to the peak temperature in the specific heat by  $\Delta = k_B T_S/0.418$ , a relation valid for a two level Schottky function<sup>22</sup>. Solving this system of two linear equations we found that  $H_{mf} = 11.4 \text{ T}$  and  $m = 0.43 \mu_B$  in  $\text{Nd}_{0.5}\text{Sr}_{0.5}\text{MnO}_3$ ,  $H_{mf} = 20.6 \text{ T}$  and  $m = 0.44 \mu_B$  in  $\text{Nd}_{0.5}\text{Ca}_{0.5}\text{MnO}_3$  and  $H_{mf} = 13.6 \text{ T}$  and  $m = 0.58 \mu_B$  in  $\text{Ho}_{0.5}\text{Ca}_{0.5}\text{MnO}_3$ . These values of  $m$  are smaller than those obtained from susceptibility measurements at high temperatures. However, they are similar to the one found by J. E. Gordon et al.<sup>9</sup> using the same method ( $H_{mf} = 10 \text{ T}$  and  $m = 0.8 \mu_B$  in  $\text{Nd}_{0.67}\text{Sr}_{0.33}\text{MnO}_3$ ).

The ground state of the  $\text{Nd}^{3+}$  and  $\text{Ho}^{3+}$  ions are usually denoted as  $^4\text{I}_{9/2}$  and  $^5\text{I}_8$ , where I stands for an orbital angular momentum  $L=6$ , the superprefix specify the total spin as  $2S + 1$  and the subscript the total angular momentum  $J$ . The number of the lowest energy levels is given by  $2J + 1$ , which leads to 5 Kramers doublets in the ground state of the first ion and a singlet and 8 Kramers doublets in the second ion<sup>21</sup>. F. Bartolomé et. al.<sup>10</sup> showed that the second doublet in the  $\text{Nd}^{3+}$  ion was approximately 120 K (in energy) above the lowest doublet. As this temperature is about 10 times higher than the temperature where the Schottky anomaly appears, the contribution of the second doublet is expected to be small. In a previous report<sup>13</sup> we showed that a two level Schottky function (only one doublet) did not fit properly our experimental data at low temperatures. The same result was verified for the new experimental data presented here. One alternative, justified by the existence of several different grains in polycrystalline samples, is to consider a distribution of energy splitting around the value that would correspond to a single crystal in the same two level Schottky model. Although the fitting results using this second approach improved a little bit, we found that they still remained unsatisfactory.

At first sight someone might be tempted to correlate the existence of the Schottky anomaly with the presence of an intrinsic magnetic moment in  $\text{Nd}^{3+}$  and  $\text{Ho}^{3+}$  ions (in contrast with  $\text{La}^{3+}$  ions without magnetic moment and no Schottky anomaly in the managanite). However, specific heat measurements reported by V. Hardy et al.<sup>28</sup> in a compound of  $\text{Pr}_{0.63}\text{Ca}_{0.37}\text{MnO}_3$  ( $\text{Pr}^{3+}$  ions have approximately the same magnetic moment as  $\text{Nd}^{3+}$  ions)

did not show any Schottky anomaly. Moreover,  $\text{Ho}^{3+}$  ions have an intrinsic magnetic moment almost 3 times bigger than  $\text{Nd}^{3+}$  ions, but the Schottky temperature at zero magnetic field were 2.73 K in  $\text{Nd}_{0.5}\text{Sr}_{0.5}\text{MnO}_3$ , 5.08 K in  $\text{Nd}_{0.5}\text{Ca}_{0.5}\text{MnO}_3$ , and 4.39 K in  $\text{Ho}_{0.5}\text{Ca}_{0.5}\text{MnO}_3$ . Probably the existence of the Schottky anomaly is related with the Kramers theorem. It states that an ion possessing an odd number of electrons, no matter how unsymmetrical the crystal field, must have a ground state that is at least doubly degenerate<sup>21</sup>. This could lead to the thermal depopulation that produces the Schottky anomaly in the specific heat. Ions of Ce, Nd, Sm, Gd, Dy, Er and Yb all have an odd number of electrons and their respective oxides present a Schottky anomaly in the specific heat. However, the Kramers theorem does not exclude that ions with an even number of electrons might also have a doubly degenerate ground state. This is the case of the Ho ions, although it is noteworthy that the magnetic entropy associated with the Schottky transition in the compound with Ho had the lowest value (see above). Besides, our results indicate that the higher  $T_S$  are found in the compounds with lower tolerance factors:  $\text{Nd}_{0.5}\text{Ca}_{0.5}\text{MnO}_3$  and  $\text{Ho}_{0.5}\text{Ca}_{0.5}\text{MnO}_3$ . The tolerance factor compares the Mn-O separation with the separation of the oxygen atom and A-site occupant in  $\text{AMnO}_3$ . In this way the tolerance factor characterizes the angle of the Mn-O-Mn bond. Compounds with higher tolerance factors present wider conduction bands, which lead to a stronger ferromagnetic interactions and lower electrical resistivity.

#### IV. CONCLUSIONS

We have made a magnetic characterization of  $\text{Nd}_{0.5}\text{Sr}_{0.5}\text{MnO}_3$ ,  $\text{Nd}_{0.5}\text{Ca}_{0.5}\text{MnO}_3$  and  $\text{Ho}_{0.5}\text{Ca}_{0.5}\text{MnO}_3$  polycrystalline samples. It allowed us to identify the ferromagnetic, anti-ferromagnetic and charge ordering phases in each case. There are two important differences among these samples. The first one is that the tolerance factor, which influences the width of the conduction band, decreases from  $\text{Nd}_{0.5}\text{Sr}_{0.5}\text{MnO}_3$  to  $\text{Ho}_{0.5}\text{Ca}_{0.5}\text{MnO}_3$ . The second one is that the rare earth ions have intrinsic magnetic moments:  $J=9/2$  for  $\text{Nd}^{3+}$  and  $J=8$  for  $\text{Ho}^{3+}$ . These intrinsic magnetic moments experience a short range order at low temperatures.

Moreover, the relation between the charge ordering temperature and the antiferromagnetic ordering temperature changes from one sample to the other. In the  $\text{Nd}_{0.5}\text{Sr}_{0.5}\text{MnO}_3$  sample they are approximately coincident ( $T_{CO} \approx T_N$ ), in the  $\text{Nd}_{0.5}\text{Ca}_{0.5}\text{MnO}_3$  sample the charge ordering temperature is much higher ( $T_{CO} \gg T_N$ ), and in the  $\text{Ho}_{0.5}\text{Ca}_{0.5}\text{MnO}_3$  sample there is no a long range antiferromagnetic transition.

We also reported, to our knowledge for the first time, specific heat measurements with applied magnetic fields between 0 and 9 T and temperatures between 2 and 300 K in all these three samples. Each curve was successfully fitted at high temperatures by an Einstein model with three optical phonon modes. Close to the charge ordering and ferromagnetic transition temperatures the specific heat curves showed peaks superposed to the characteristic response of the lattice oscillations. The entropy variation corresponding to the charge ordering transition was higher than the one corresponding to the ferromagnetic transition. Near 160 K in the two compounds with  $\text{Nd}^{3+}$  ions the specific heat curve showed an abrupt change in slope, which were correlated to the corresponding antiferromagnetic transition.

Absolute values of specific heat close to 2 K were about 100 times higher in our samples than in other charge ordering samples like  $\text{Pr}_{0.63}\text{Ca}_{0.37}\text{MnO}_3$ . At low temperatures the specific heat curve, in all three studied samples and measured magnetic fields, showed a Schottky-like anomaly. In all cases an increase in the applied magnetic field moves the Schottky peak to higher temperatures. However, the height of the peak and the entropy, behave differently in  $\text{Nd}_{0.5}\text{Sr}_{0.5}\text{MnO}_3$  than in the other two samples. We could not successfully fit the curves by either assuming a singlet or a distribution of two-level-Schottky anomaly. Besides, we did not find a straightforward correlation between the maximum temperature of the Schottky anomaly and the magnetic moment of the rare earth ions. More experiments are clearly necessary to unambiguously identify the origin of the Schottky anomaly and its possible correlation with the charge ordered phase.

We thank the Brazilian science agencies FAPESP and CNPq for the financial support.

## FIGURE CAPTIONS

Figure 1. Temperature dependence of the magnetization, with a 5 T applied magnetic field, in field cooling–warming condition for the three polycrystalline samples studied. Magnetization is given in Bohr magnetons per manganese ion. It is indicated  $T_C$ ,  $T_N$  and  $T_{CO}$  for in each sample. Note that charge ordering can occur in the presence of a ferromagnetic, antiferromagnetic or a paramagnetic phase.

Figure 2. Inverse of DC susceptibility measurements as a function of temperature in the  $\text{Ho}_{0.5}\text{Ca}_{0.5}\text{MnO}_3$  sample. The main graph shows the measurement made with a 5 T applied magnetic field, while the inset with a probe magnetic field of 0.1 mT. Lines are only guides to the eye.

Figure 3. Magnetization versus applied magnetic field at 2 K for the three samples studied. After a zero field cooling the magnetic field was increased from 0 to 5 T, decreased from 5 T to -5 T and increased again from -5 T to 5 T. The solid line represents a fitting by a Brillouin function (See the text for details). Magnetization is given in Bohr magnetons per manganese ion.

Figure 4. Specific heat measurements with zero magnetic field from 2 to 300 K for  $\text{Nd}_{0.5}\text{Sr}_{0.5}\text{MnO}_3$  (open squares),  $\text{Nd}_{0.5}\text{Ca}_{0.5}\text{MnO}_3$  (closed circles) and  $\text{Ho}_{0.5}\text{Ca}_{0.5}\text{MnO}_3$  (open triangles). Continuous lines represent the fitting of the phonon background to the Einstein model (see text). The  $\text{Nd}_{0.5}\text{Sr}_{0.5}\text{MnO}_3$  and  $\text{Ho}_{0.5}\text{Ca}_{0.5}\text{MnO}_3$  curves were displaced 20 J/mol K upside and downside, respectively.

Figure 5. Differences between the experimental specific heat data and the corresponding phonon background curves in the  $\text{Nd}_{0.5}\text{Sr}_{0.5}\text{MnO}_3$  sample (open squares),  $\text{Nd}_{0.5}\text{Ca}_{0.5}\text{MnO}_3$  sample (closed circles) and  $\text{Ho}_{0.5}\text{Ca}_{0.5}\text{MnO}_3$  sample (open triangles).

Figure 6. Specific heat measurements between 2 and 30 K in the samples of (a)  $\text{Nd}_{0.5}\text{Sr}_{0.5}\text{MnO}_3$ , (b)  $\text{Nd}_{0.5}\text{Ca}_{0.5}\text{MnO}_3$  and (c)  $\text{Ho}_{0.5}\text{Ca}_{0.5}\text{MnO}_3$ . Measurements were made in

the presence of applied magnetic fields of 0 T (open squares), 5 T (closed circles), 7 T (open up triangles) and 9 T (closed down triangles). Continuous lines represent the fitting of the 15 to 30 K temperature interval data to the phonon contribution, as it is explained in the text. The graphs in the insets show the difference between the experimental values and the extrapolation of the phonon contribution to temperatures lower than 15 K.

Figure 7. Debye temperature ( $T_D$ ), entropy variation between 2 and 20 K ( $\Delta S$ ) and Schottky temperature ( $T_S$ ) as a function of the applied magnetic field in  $\text{Nd}_{0.5}\text{Sr}_{0.5}\text{MnO}_3$  (open squares),  $\text{Nd}_{0.5}\text{Ca}_{0.5}\text{MnO}_3$  (closed circles) and  $\text{Ho}_{0.5}\text{Ca}_{0.5}\text{MnO}_3$  (open triangles).

## REFERENCES

- <sup>1</sup> P. G. Radaelli, D. E. Cox, M. Marezio and S-W. Cheong, Phys. Rev. B 55 (5) 3015 (1997)
- <sup>2</sup> Guo-meng Zhao, K. Ghosh and R. L. Greene, J. Phys.: Condens. Matter 10, L737 (1998)
- <sup>3</sup> Y. Moritomo, Phys. Rev. B 60 (14) 10374 (1999)
- <sup>4</sup> Gang Xiao, G. Q. Gong, C. L. Canedy, E. J. McNiff, Jr. and A. Gupta, J. Appl. Phys. 81 (8) 5324 (1997)
- <sup>5</sup> S. Mori, C. H. Chen and S.-W. Cheong, Nature 392, 473 (1998)
- <sup>6</sup> Myron B. Salamon and Marcelo Jaime, Reviews of Modern Physics 73, 583 (July 2001)
- <sup>7</sup> J. López, P. N. Lisboa-Filho, W. A. C. Passos, W. A. Ortiz and F. M. Araujo-Moreira, Journal of Magnetism and Magnetic Materials 226-230, 507-508 (2001). Also at <http://arXiv.org/abs/cond-mat/0004460>
- <sup>8</sup> J. López, P. N. Lisboa Filho, W. A. C. Passos, W. A. Ortiz, F. M. Araujo-Moreira, Kartik Ghosh, O. F. de Lima and D. Schaniuel, Phys. Rev. B 63 (22) 224422 (9 pages) 2001. Also at <http://arxiv.org/abs/cond-mat/0103305>
- <sup>9</sup> J. E. Gordon, R. A. Fisher, Y. X. Jia, N. E. Phillips, S. F. Reklis, D. A. Wright and A. Zettl, Phys. Rev. B 59 (1) 127 (1999)
- <sup>10</sup> Fernando Bartolomé, Juan Bartolomé, Miguel Castro and Julio J. Melero, Phys. Rev. B 62 (2) 1058 (2000)
- <sup>11</sup> V. N. Smolyaninova, K. Ghosh and R. L. Greene, Phys. Rev. B 58 (22) R14725 (1998)
- <sup>12</sup> V. N. Smolyaninova, Amlan Biswas, X. Zhang, K. H. Kim, Bog-Gi Kim, S-W. Cheong and R. L. Greene, Phys. Rev. B 62 (10) R6093 (2000)
- <sup>13</sup> J. López, P. N. Lisboa-Filho, O. F. de Lima and F. M. Araujo-Moreira, in press, Journal of Magnetism and Magnetic Materials (2001). Also at <http://arXiv.org/abs/cond->

mat/0105571

- <sup>14</sup> Lisboa Filho, P. N., S. M. Zanetti, E. R. Leite and W. A. Ortiz, *Materials Letters* 38 (4), 289 (1999)
- <sup>15</sup> R. Kajimoto, H. Eoshizawa, H. Kawano, H. Kuwahara, Y. Tokura, K. Ohoyama e M. Ohashi, *Phys. Rev. B* 60 (13) 9506 (1999)
- <sup>16</sup> F. Millange, S. de Brion and G. Chouteau, *Phys. Rev. B* 62 (9) 5619 (2000)
- <sup>17</sup> T. Terai, T. Sasaki, T. Kakeshita, T. Fukuda, T. Saburi, H. Kitagawa, K. Kindo and M. Honda, *Phys. Rev. B* 61 (5) 3488 (2001)
- <sup>18</sup> R. Mathieu, P. Nordblad, A. R. Raju e C. N. R. Rao, <http://arxiv.org/abs/cond-mat/0106606> (2001)
- <sup>19</sup> M. T. Causa, M. Tovar, A. Caneiro, F. Prado, G. Ibañes, C. A. Ramos, A. Butera, B. Alascio, X. Obradors, S. Piñol, F. Rivadulla, C. Vázquez-Vázquez, M. A. López-Quintela, J. Rivas, Y. Tokura and S. B. Oseroff, *Phys. Rev. B* 58 (6) 3233 (1998)
- <sup>20</sup> R. Mahendiran, M. R. Ibarra, A. Maignan, F. Millange, A. Arulraj, R. Mahesh, B. Raveau and C. N. R. Rao, *Phys. Rev. Lett.* 82 (10) 2191 (1999)
- <sup>21</sup> Neil W. Ashcroft and N. David Mermin, "Solid State Physics", Saunders College Publishing (1975)
- <sup>22</sup> C. Kittel, "Introduction to Solid State Physics", fifth edition, New York; London :J. Wiley (1976)
- <sup>23</sup> A. P. Ramirez, P. Schiffer, S-W. Cheong, C. H. Chen, W. Bao, T. T. M. Palstra, P. L. Gammel, D. J. Bishop and B. Zegarski, *Phys. Rev. Lett.* 76 (17) 3188 (1996)
- <sup>24</sup> A. K. Raychaudhuri, Ayan Guha, I. Das, R. Rawat and C.N.R. Rao, available in <http://arxiv.org/abs/cond-mat/0105384>

- <sup>25</sup> V. Dediú, C. Ferdeghini, F. C. Maticotta, P. Nozar and G. Ruani, *Phys. Rev. Lett.* 84 (19) 4489 (2000)
- <sup>26</sup> E. Granado, A. García, J. A. Sanjurjo, C. Rettori and I. Torriani, *Phys. Rev. B* 63, 064404 (2001)
- <sup>27</sup> Susumu Shimomura, Keisuke Tajima, Nobuyoshi Wakabayashi, Shiho Kobayashi, Hideki Kuwahara and Yoshinori Tokura, *J. Phys. Soc. Japan* 68 (6), 1943 (1999)
- <sup>28</sup> V. Hardy, A. Wahl, C. Martin and Ch. Simon, *Phys. Rev. B* (63) 224403 (2001)
- <sup>29</sup> J. J. Hamilton, E. L. Keatley, H. L. Ju, A. K. Raychaudhuri, V. N. Smolyaninova e R. L. Greene, *Phys. Rev. B* 54 (21) 14926 (1996)
- <sup>30</sup> J. López and O. F. de Lima, unpublished (2002).
- <sup>31</sup> Y. S. Touloukian and E. H. Buyco, *Thermophysical Properties of Matter Specific heat Nonmetallic Solids* (1970)
- <sup>32</sup> H. Kawano, R. Kajimoto, H. Eoshizawa, E. Tomioka, H. Kuwahara and E. Tokura, *Phys. Rev. Lett.* 78, 4253 (1997)

Figure 1

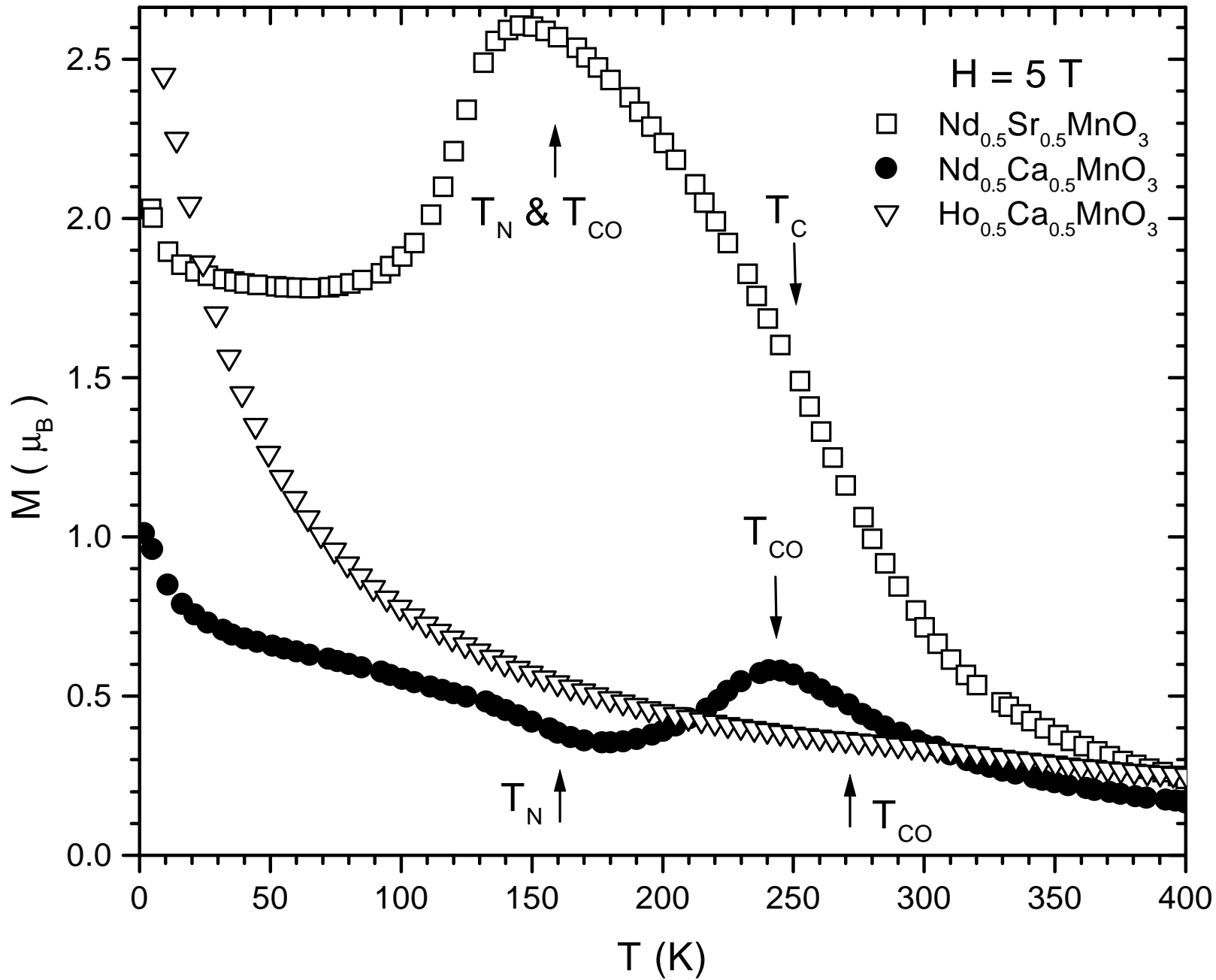


Figure 2

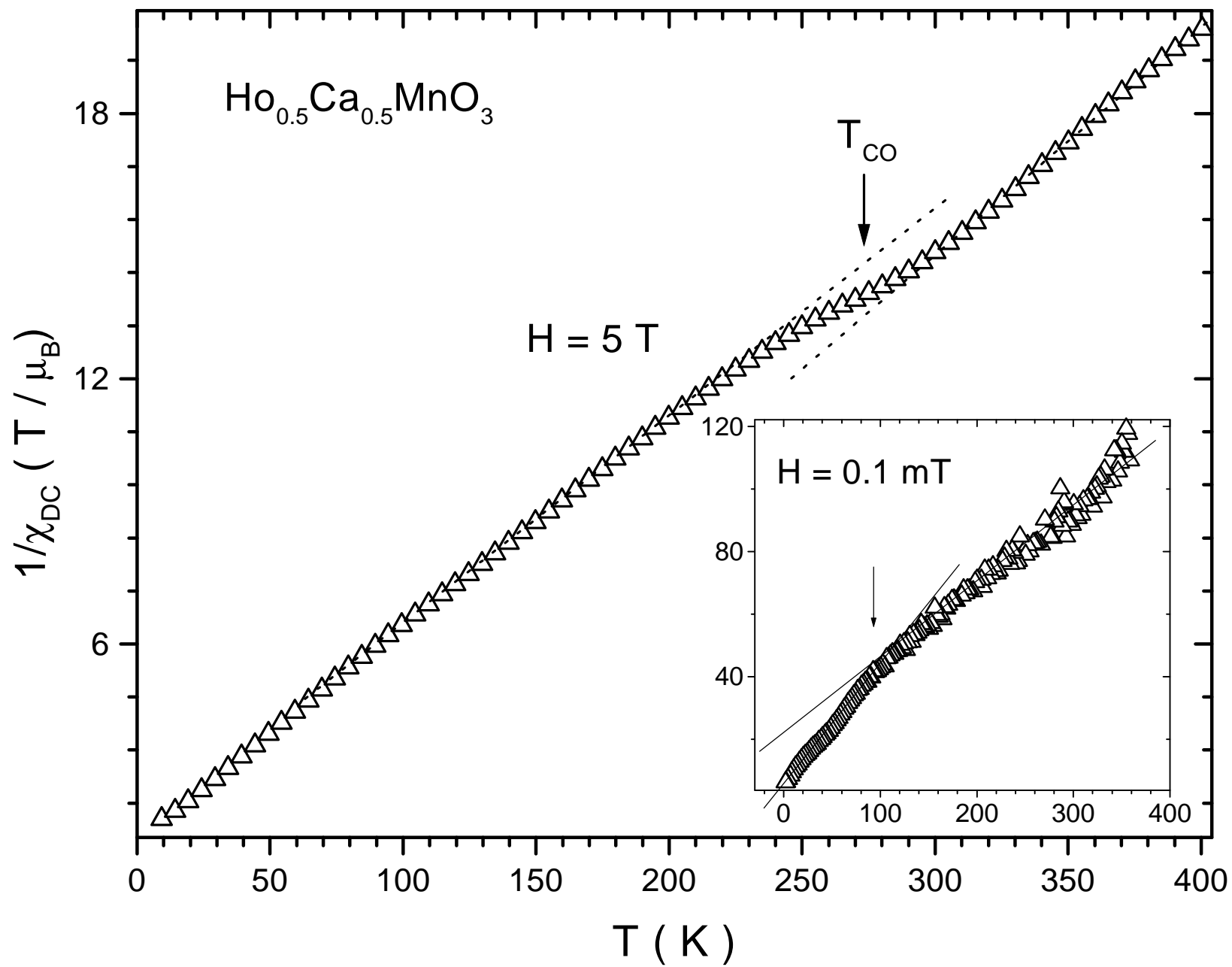


Figure 3

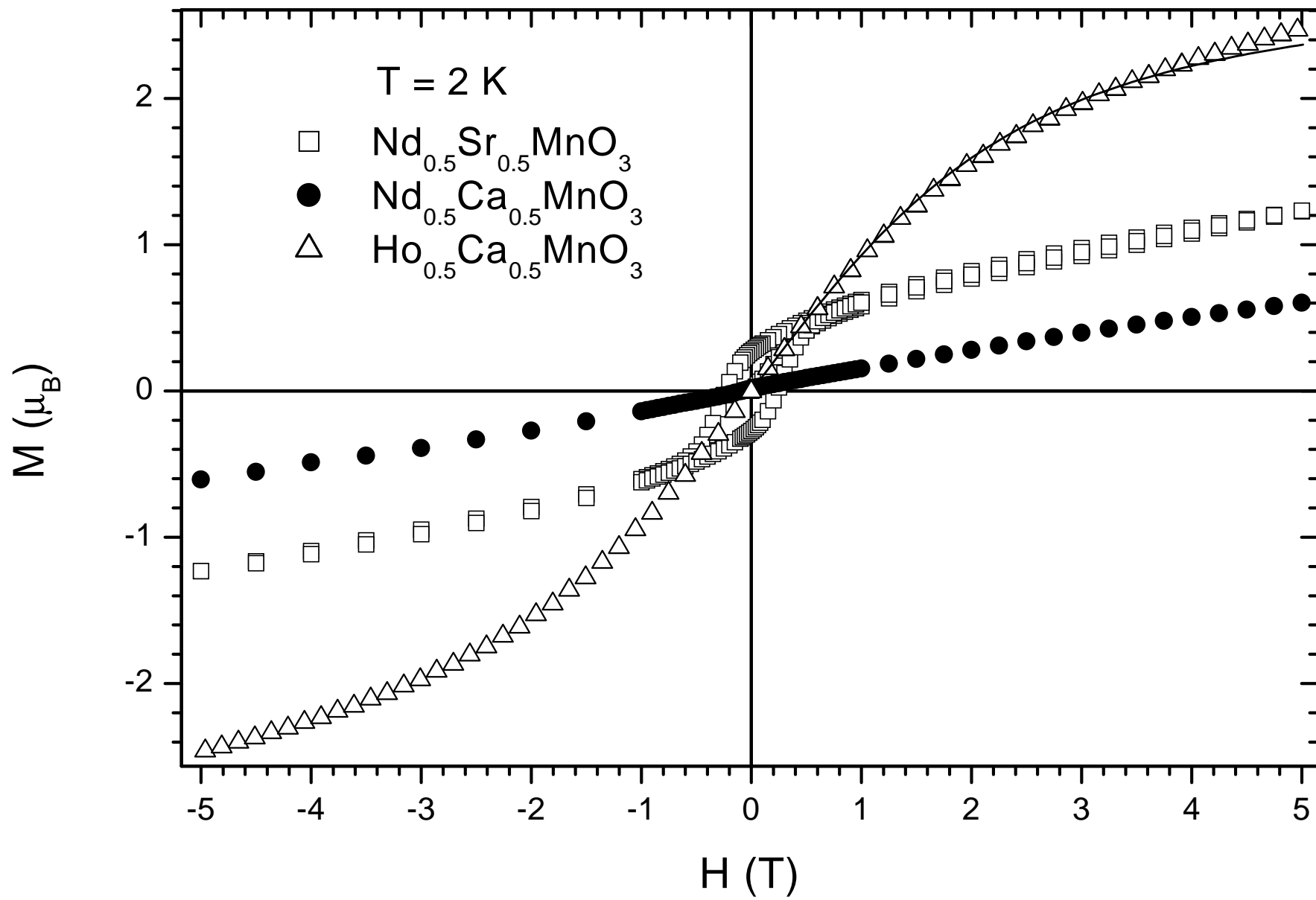


Figure 4

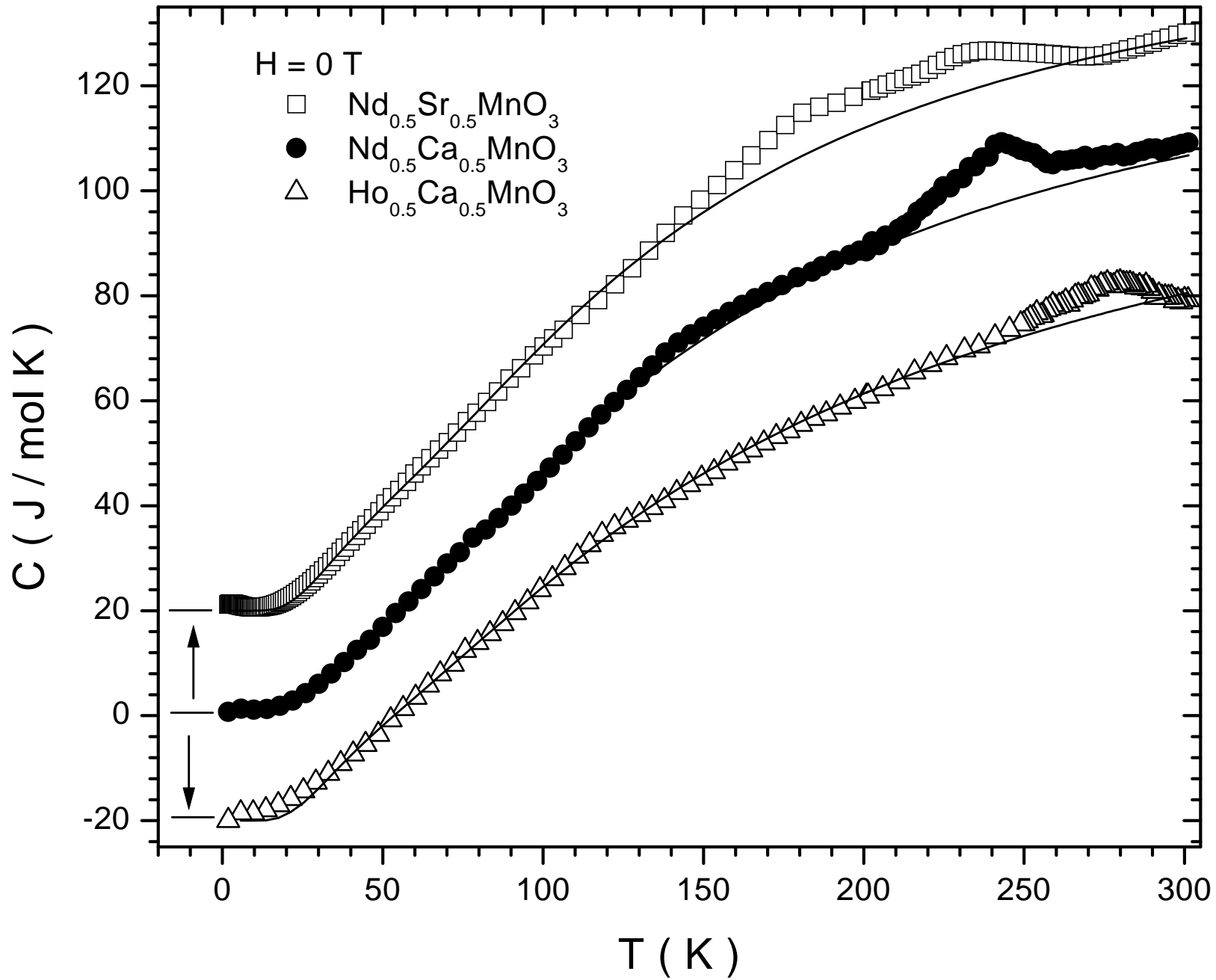


Figure 5

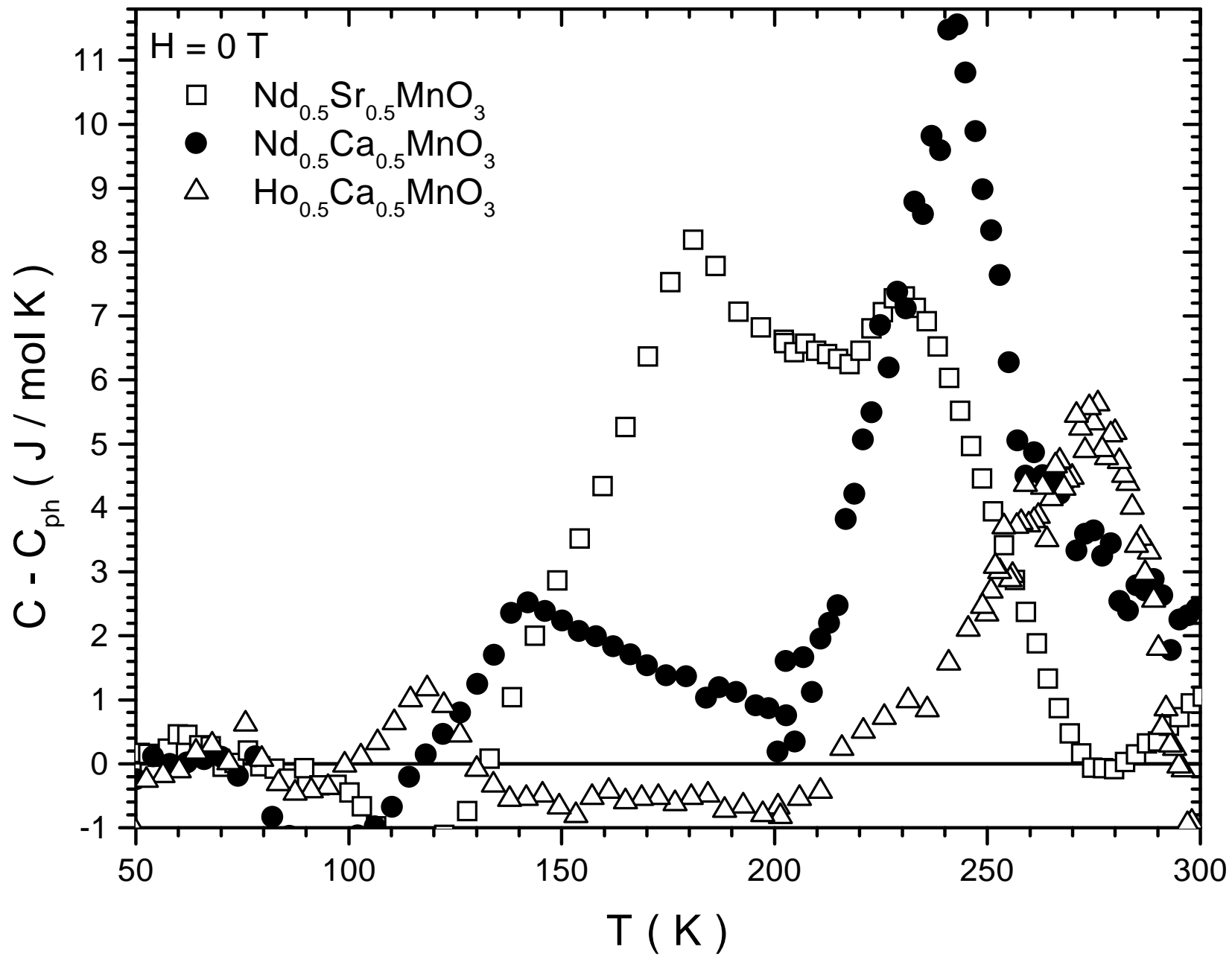


Figure 6a

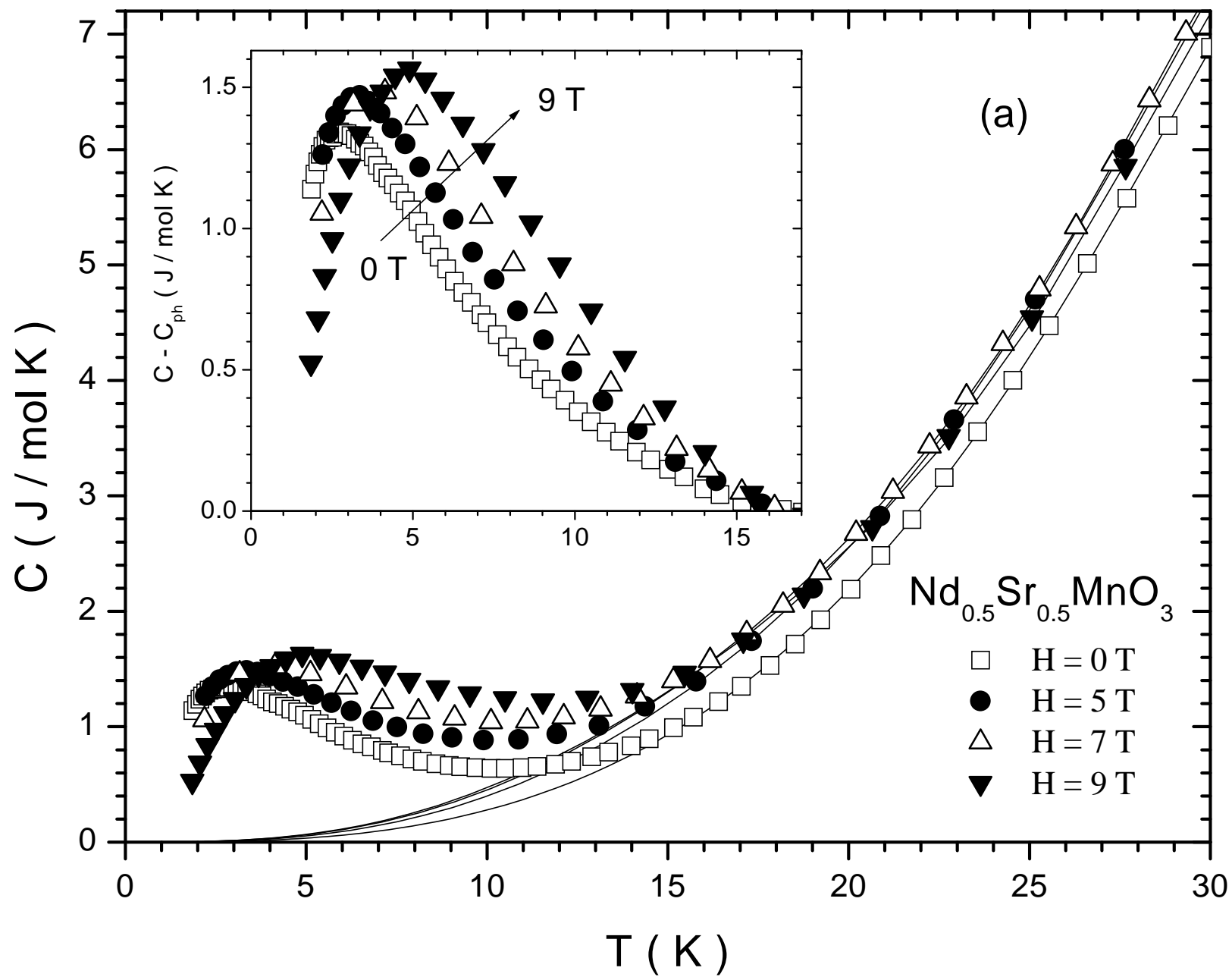


Figure 6b

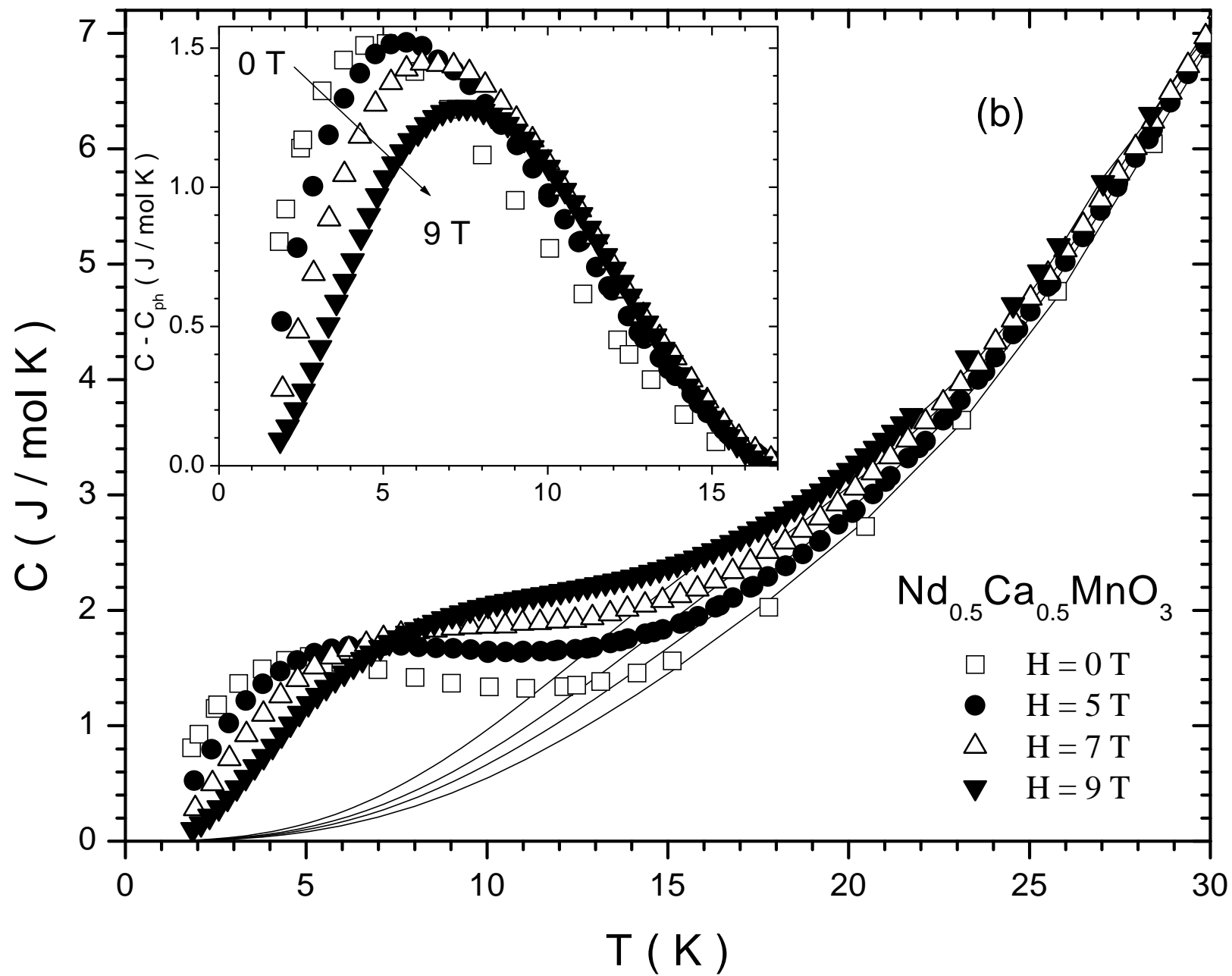


Figure 6c

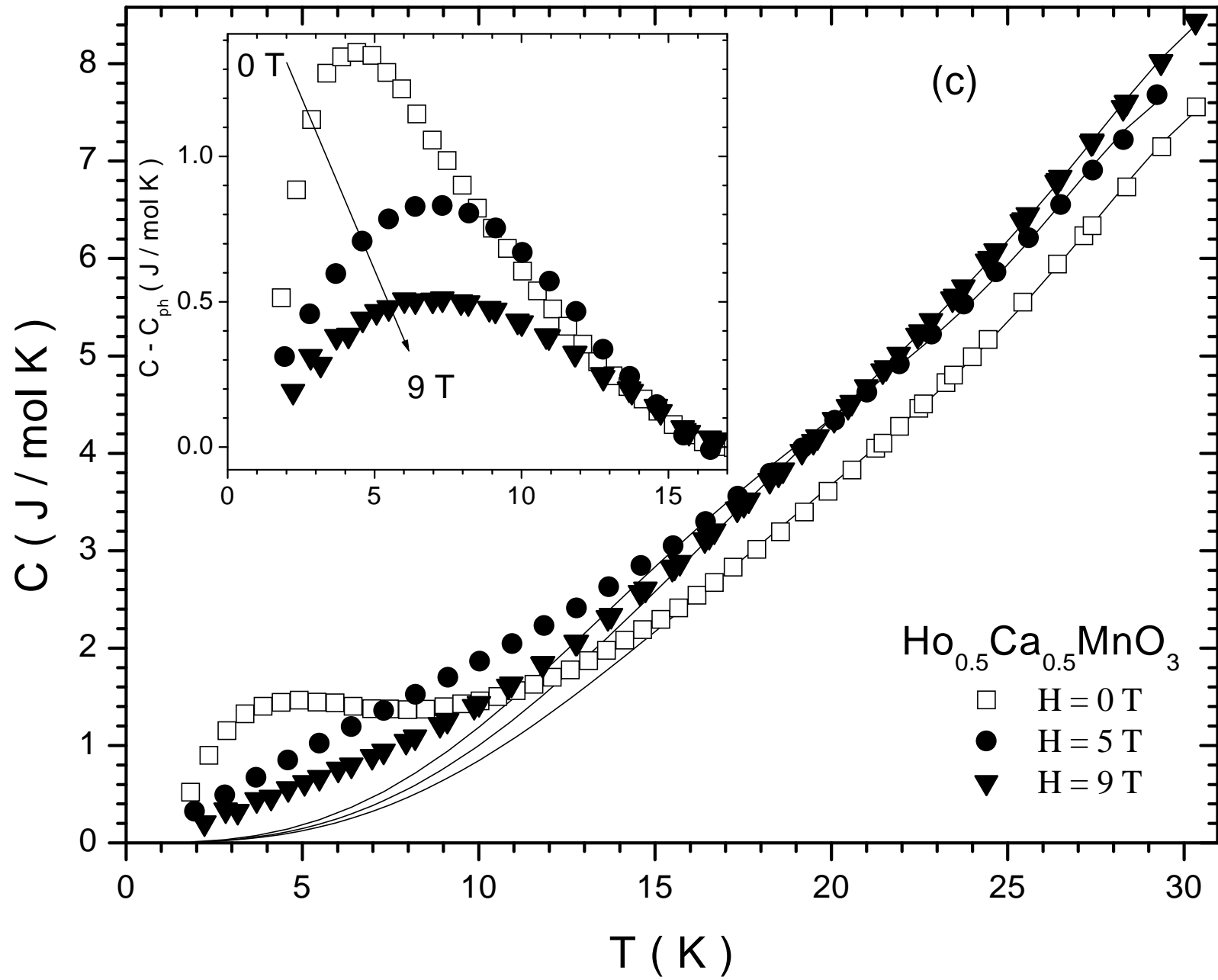


Figure 7

